

Application of the VMM ASIC for SiPM-based calorimetry

**I. Bearden^a V. Buchakchiev^{b,*} A. Buhl^a L. Dufke^a T. Isidori^c S. Jia^a V. Kozhuharov^b
C. Loizides^d H. Muller^{e,f} D. Pfeiffer^{e,g} M. Rauch^h A. Rusu^{d,i} R. Simeonov^b**

^a*University of Copenhagen, Copenhagen, Denmark*

^b*Faculty of Physics, University of Sofia, Sofia, Bulgaria*

^c*The University of Kansas, Lawrence, USA*

^d*ORNL, Oak Ridge, USA*

^e*European Organization for Nuclear Research (CERN), 1211 Geneva 23, Switzerland*

^f*Physikalisches Institut, University of Bonn, Nußallee 12, 53115 Bonn, Germany*

^g*European Spallation Source ERIC (ESS), Box 176, SE-221 00 Lund, Sweden*

^h*University of Bergen, Bergen, Norway*

ⁱ*SRS Technology, 30 Promenade des Artisans, 1217 Meyrin, Switzerland*

*E-mail: *valentin@phys.uni-sofia.bg*

ABSTRACT: Highly integrated multichannel readout electronics is crucial in contemporary particle physics experiments. A novel silicon photomultiplier readout system based on the VMM3a ASIC was developed, for the first time exploiting this chip for calorimetric purposes. To extend the dynamic range the signal from each SiPM channel was processed by two electronics channels with different gain. A fully operational prototype system with 256 SiPM readout channels allowed the collection of data from a prototype of the ALICE Forward Hadron Calorimeter (FoCal-H). The design and the test beam results using high energy hadron beams are presented and discussed, confirming the applicability of VMM3a-based solutions for energy measurements in a high rate environment.

Contents

1	Introduction	1
2	Experimental setup	2
3	Data analysis	5
4	Conclusion	8

1 Introduction

ALICE FoCal [1, 2] is a forward calorimeter which will be installed during the Long Shutdown 3 (LS3) of the Large Hadron Collider (LHC) at CERN, and will start taking data during LHC Run 4. Several testing campaigns addressed the design and the physics performance of prototypes of the electromagnetic (FoCal-E) and the hadronic (FoCal-H) sections of FoCal [3]. In addition, various readout systems were used with the FoCal-H prototypes. The present study addresses the compatibility between the FoCal-H Prototype 2 and the SRS (Scalable Readout System) with the VMM Hybrid front-end electronics.

The SRS [4, 5] is a versatile and highly adaptable solution for data transfer between detectors and computers. The system was developed by the RD51 Collaboration and allows use with detectors of any size while also lowering costs due to only part of the system requiring redevelopment for new applications. As part of the NSW (New Small Wheel) upgrade on the ATLAS experiment, the SRS system was used to implement new specially developed ASIC, the VMM3a [6, 7], to replace the original APV25 readout chips [8].

A VMM ASIC has 64 channels each with its own preamplifier, shaper, peak detector and ADCs. The chip can be programmed for multiple applications as its gain, polarity, peaking time, threshold and timing precision are all adjustable. It was originally developed for use with Micromega and GEM gaseous detectors and is tailored towards high event rates with low channel activation rates per event. FoCal-H prototype is designed as a plastic-absorber calorimeter with a SiPM-based light detection. The expected event rate during test beam campaigns is of the order of 10 kHz, but a large number of channels are activated for each event. Due to the hadronic shower's geometry, most of the activated channels are usually connected to a single readout chip, leading to a high and non-uniform load. In this paper we present the results of an R&D study of the usage of the VMM with one of the FoCal-H prototypes which may extend the applicability of the VMM ASIC to SiPM-based calorimeters in general.

2 Experimental setup

The FoCal-H prototype consists of 9 modules with dimensions $6.5 \times 6.5 \times 110 \text{ cm}^3$ in a 3×3 arrangement. Each module consists of 24×28 copper tubes with scintillating fibers inside them, with 4 tubes removed for the installation of supporting rods. Light detection is provided by Hamamatsu S13360-6025PE SiPMs. The 668 fibers of each module are split into bundles. The outer 8 modules of the prototype are split into 25 channels with ~ 27 fibers per channel. The central one which detects the most energy is split into 49 channels with ~ 14 fibers per channel.

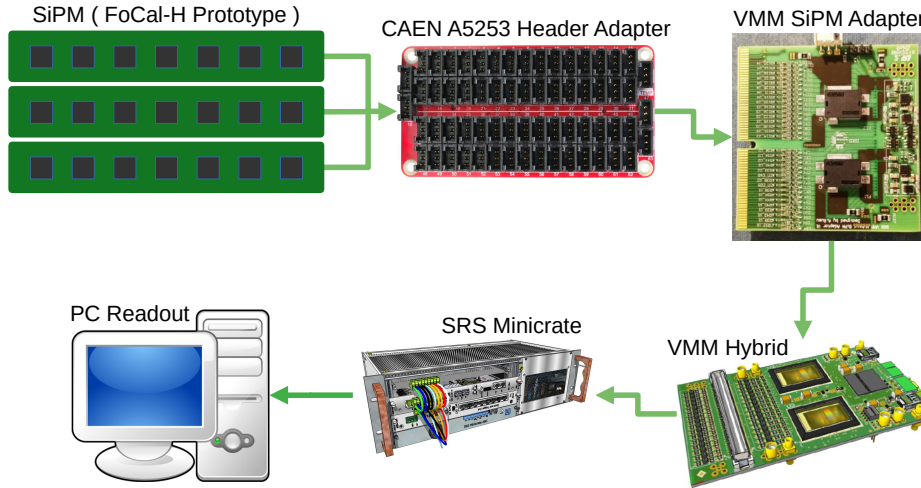


Figure 1. Schematic representation of the full readout setup.

The FoCal-H prototype equipped with 4 VMM Hybrids was tested at the SPS accelerator complex at CERN. The readout setup is presented in Figure 1. It consists of the following major components:

- The Focal-H prototype: It is represented by the Silicon Photomultipliers.
- CAEN A5253 header adapter: For facilitation, and independently of the readout system, the SiPMs outputs from the FoCal-H back panel were connected to the CAEN A5253 64 channel header adapter [9].
- The VMM SiPM adapter board: To test the VMM readout solution with Silicon Photomultipliers, a dedicated SiPM adapter board was developed in collaboration with RD51 [10] which can be plugged into the CAEN adapter. It acts as a 128 channel interface from the FoCal-H detector to the RD51 VMM hybrid. A prototype was used in the FoCal test beam.
- RD51 VMM hybrid: The VMM hybrid board, shown in figure 2, right, houses two VMM3a ASICs, for a total of 128 electronics channels. A Xilinx Spartan-6 Field Programmable Gate Array (FPGA) ensures the ASIC configuration and the communication (including hit data transfer) with the SRS system via micro HDMI connectors [11].

- SRS minicrate: The SRS back-end, as described in [4], is contained in the SRS minicrate. It acts as a data aggregator and is able to serve up to 8 hybrid boards connected via HDMI interface. The SRS system also adds coarse timing information for time stamp calculations, and pads then feeds the data to the readout PC.
- PC Readout: A standard PC is used. The PC allows the configuration of the SRS readout by setting various parameters such as thresholds, gains, etc. The data, which is sent by the SRS system via a UDP protocol, is recorded by filtering the incoming network stream, and further storing it on disk for processing.

The SiPM Adapter board is shown in Figure 2. It transforms the SiPM signal risetime into charge and houses 2 bias voltage generators which can provide between 0 V and 85 V (programmable through an I2C interface). The HV distribution is split into 2 regions of 32 SiPMs which in the prototype, have the same bias voltage. The adapter uses a precise DAC capable of adjusting the SiPM bias voltage in steps of 5 mV. It also has an ADC to measure the actually provided voltages and currents for the two regions.

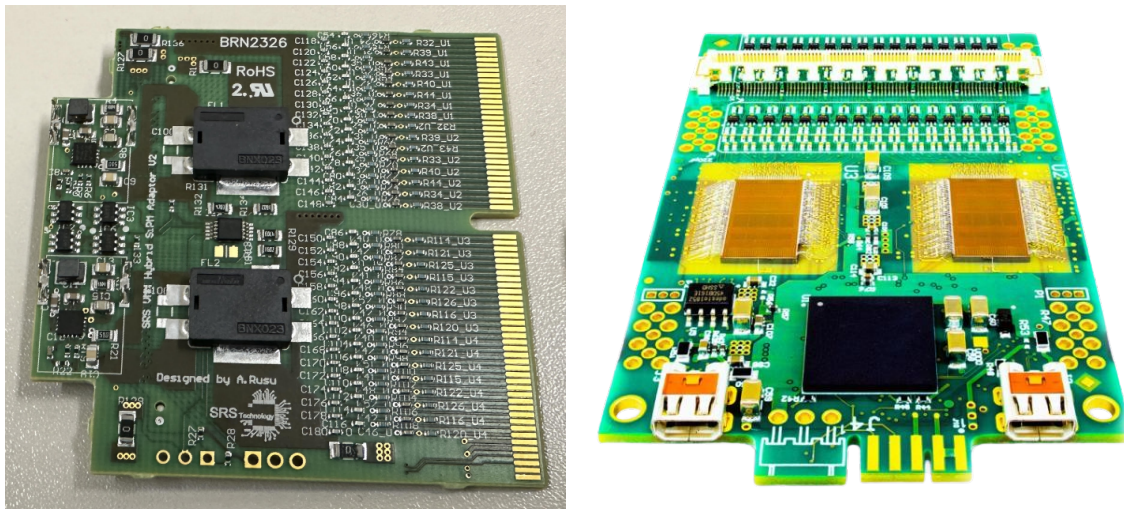


Figure 2. Left - A photograph of the SiPM adapter board which allows the connection between the VMM Hybrid and the SiPMs through the CAEN A5253 header adapter. Right - The VMM Hybrid board which houses and configures the VMM ASICs.

Initially, with the first prototype of the VMM SiPM adapter board, only 32 channels per VMM (out of 64) were connected to the FoCal-H. However, after testing the FoCal-H prototype with a hadron beam at CERN SPS, due to problems with ADC saturation, it was decided to make use of the remaining 32 channels per VMM chip as Low(er) Gain channels. Therefore, the SiPM adapter board aims to extend the original dynamic range of the VMM through the use of charge division coupling with the same amplifier gain, resulting in High Gain (HG) and Low Gain (LG) channels. With this setup each SiPM channel is connected to two VMM channels through identical amplifier circuits with the only exception being their coupling capacitors, as can be seen in Figure 3.

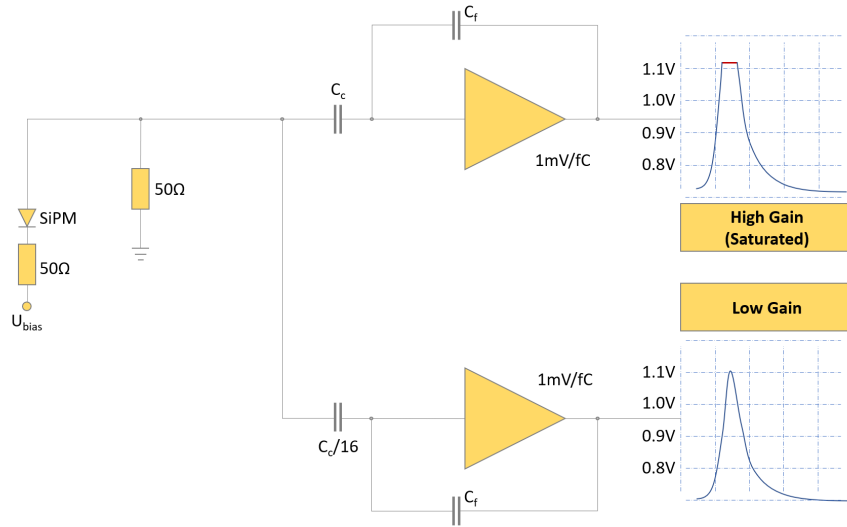


Figure 3. The circuit on the VMM SiPM adapter board which extends the dynamic range by splitting the SiPM signal into High Gain and Low Gain electronics channels.

The chosen values of the capacitors are in a 16:1 ratio, resulting in the same 16:1 ratio in the VMM output analog signals, thus giving at least one non-saturated output for input signals with much larger amplitudes.

Eight VMM chips were used to cover the 249 channels of the detector, with each detector channel being digitized by two VMM channels - one HG and one LG. The VMM connected to the back of the FoCal-H is presented in Figure 4 along with a visualisation of the beam profile using this setup with a 350 GeV hadron beam. The detector was moved such that the center of the beam was inside the lower left prototype module, as visible on the plot.

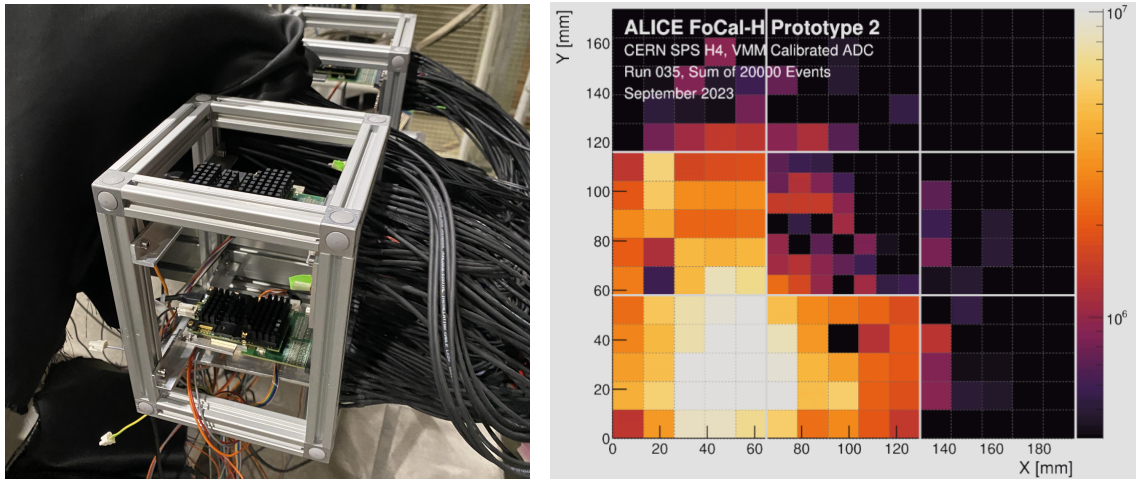


Figure 4. Left - VMM Hybrids connected to the back of the FoCal-H prototype through the SiPM adapter boards. Right - Cumulative charge in each FoCal-H channel in ADC units for 350 GeV beam energy.

Eighty-seven separate runs were performed using both hadron and electron beams pointing towards the central module of the FoCal-H prototype. The hadron beam energy was varied between 60 GeV and 350 GeV. Data for different gain and SiPM bias voltage was also collected for some of the available energies.

3 Data analysis

A single data unit of the VMM is called a hit and is described by a 38 bit binary sequence in the stored data. The first 2 bits are flags. The 3rd through 8th bits provide the channel ID (values from 0 to 63); next 10 bits contain the digitized charge value; 8 bits a reserved for the TDC value and the last 12 bits - for the bunch-crossing ID (BCID) [7].

The time stamp for each hit is calculated based on the BCID, the TDC and the so-called FEC markers as described in [7]. Afterwards, the stream is processed by bunching hits within an 8 μ s time window. Each such cluster is defined as a single event. The total reconstructed charge is computed defined as the sum total ADC units for all activated HG channels in the event:

$$Q_{\text{event}}^{\text{HG}} = \sum_i^N \text{ADC}_i^{\text{HG}} \quad (3.1)$$

where N is the number of the in-time hits. In order to suppress noise, events with $N < 6$ are rejected.

The distributions of $Q_{\text{event}}^{\text{HG}}$ in ADC units for data collected with different beam energies is presented in Figure 5.

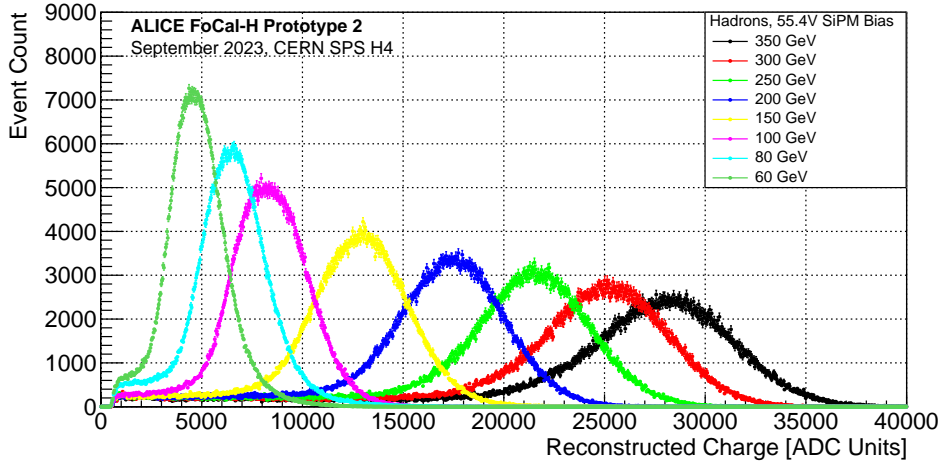


Figure 5. Comparison of the total charge distributions for all available beam energies between 60 GeV and 350 GeV. Distributions are normalised by the total number of events. SiPM bias voltage set to 55.4 V.

Due to the limited ADC range some of the channels in an event may saturate ($\text{ADC}_i^{\text{HG}} = 1023$). The mean number of saturated HG channels per event as a function of the beam energy is shown on Figure 6. Even for low beam energies ($E_{\text{beam}} \leq 100$ GeV) the mean number of saturated channels is around one and above which indicates that the central channel almost always saturates. The

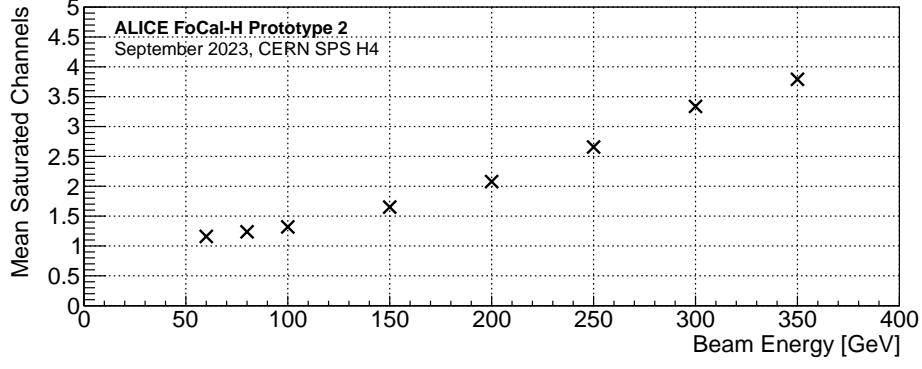


Figure 6. The mean number of saturated HG channels per event as a function of the beam energy. SiPM bias voltage set to 55.4 V.

ADC saturation affects the linearity of the charge reconstruction, as shown in Figure 7 where the dependence of $Q_{\text{event}}^{\text{HG}}$ is plotted as a function of the beam energy. A linear fit is made using the data points with beam energy from 60 GeV to 150 GeV and the line is extrapolated to cover the full energy range. The bottom plot shows the ratio between the reconstructed charge and the expected charge (from the linear fit). It can be seen that for beam energies of 250 GeV and higher the departure from linearity is larger than 2% and even reaches 10% at 350 GeV.

The saturation problem is addressed by adopting a charge reconstruction method using a combination of the LG and the HG channels (chapter 2). In the range where a signal is present in both the HG and the LG components of a channel, a calibrating equation is extracted through a linear fit to the correlation between the recorded values for HG and LG. This calibration is performed separately for each channel. The linear correlation is assumed to be respected in the range beyond HG saturation and is extrapolated.

A new “combined” ADC value $\text{ADC}_i^{\text{MIX}}$ is defined as

$$\text{ADC}_i^{\text{MIX}} = k_i * \text{ADC}_i^{\text{LG}} + c_i \quad (3.2)$$

when an HG channel is saturated and data in the corresponding LG channel is available (with k_i and c_i being the channel-by-channel calibration parameters), and

$$\text{ADC}_i^{\text{MIX}} = \text{ADC}_i^{\text{HG}} \quad (3.3)$$

when the HG channel is not saturated, or there is no available LG channel data. The final event charge is calculated as

$$Q_{\text{event}}^{\text{MIX}} = \sum_i^N \text{ADC}_i^{\text{MIX}}. \quad (3.4)$$

Thus, whenever LG data is available, and the corresponding HG channel is saturated, we calculate a rescaled ADC value for the HG charge from the LG data, and use that for our reconstruction, effectively increasing the dynamic range. The effect of such a calibration can be seen in Figure 8 where the distribution of $(Q_{\text{event}}^{\text{HG}})$ is compared to the distribution of $Q_{\text{event}}^{\text{MIX}}$ for 200 GeV. Usage of the rescaled LG values instead of the saturated HG values induces a shift of the total reconstructed

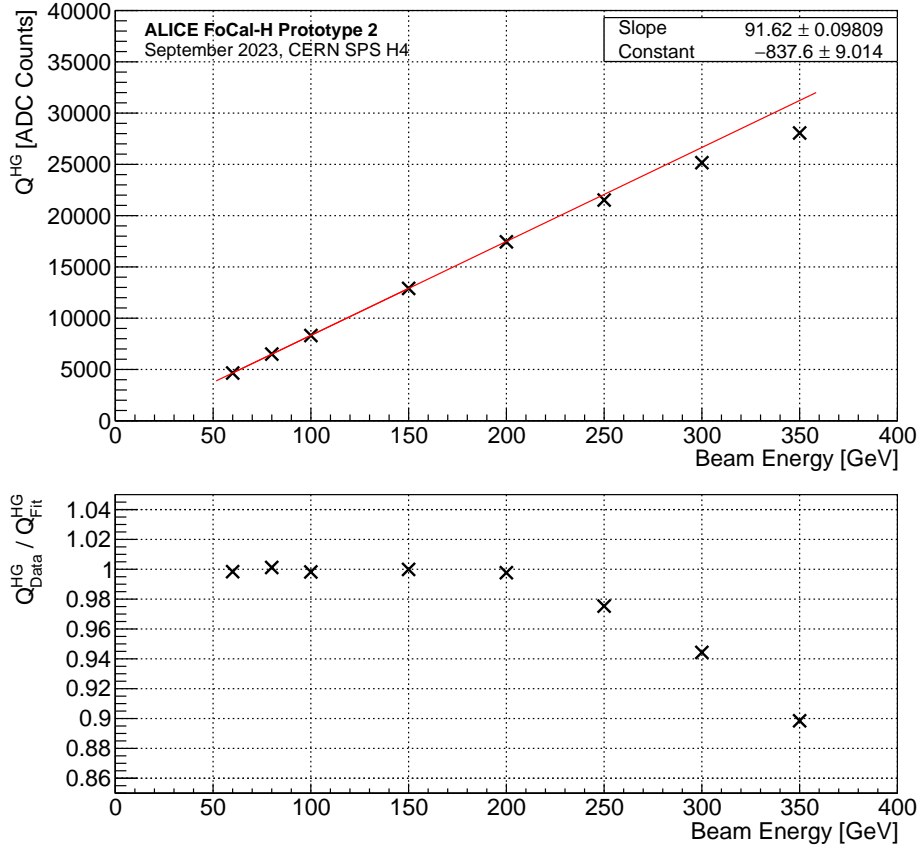


Figure 7. Top panel: Dependence of the mean values of Q^{HG} as a function of the hadron beam energy. Bottom panel: Ratio between the mean values of Q^{HG} and the values predicted by the fit as a function of the hadron beam energy. SiPM bias voltage set to 55.4 V.

charge by about 4.7%. The relative resolution $\sigma(Q)/Q$ increases from 14.8% for $Q^{\text{HG}}_{\text{event}}$ to 16.6% for $Q^{\text{MIX}}_{\text{event}}$.

The dependence of the mean of $Q^{\text{MIX}}_{\text{event}}$ as a function of the beam energy is presented on Figure 9 (top). Again, a linear fit is performed for the energy range 60 GeV to 150 GeV, and the function is extrapolated to 350 GeV. In the ratios between the reconstructed $Q^{\text{MIX}}_{\text{event}}$ and the fit prediction shown on Figure 9 (bottom) the departure from linearity reaches 2% at the 300 GeV data point compared to 250 GeV when only using HG. A loss of linearity is still observed even though the LG channels do not saturate. This could be due to transversal and longitudinal shower leakage due to the finite dimensions of the FoCal-H prototype and to saturation before the digitization stage at the VMM.

While not being the main focus of the presented study, the dependence of the relative energy resolution ($\sigma(Q^{\text{MIX}}_{\text{event}})/Q^{\text{MIX}}_{\text{event}}$) is presented in Figure 10 as a function of the beam energy.

The energy dependence of the resolution is approximated using

$$\frac{\sigma(Q)}{Q} = \frac{A}{\sqrt{E}} \oplus \frac{B}{E} \oplus C \quad (3.5)$$

where A is the term describing stochastic effects, B is the noise term relating to the readout

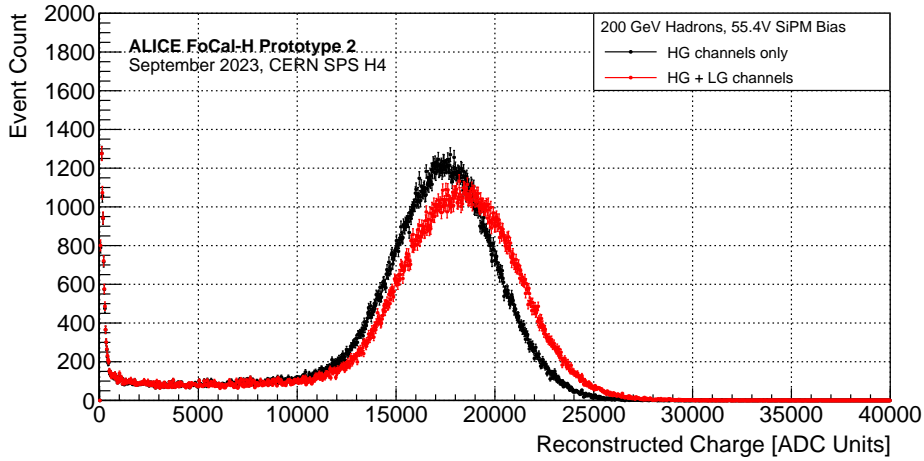


Figure 8. Comparison between reconstructed charge distributions using $Q_{\text{event}}^{\text{HG}}$ and $Q_{\text{event}}^{\text{MIX}}$, showing the resultant shift towards larger reconstructed charge when $Q_{\text{event}}^{\text{MIX}}$ is used. Distributions are normalised by the total number of events.

electronics and C is the constant term relating to shower leakage and miscalibration effects. The obtained values for the resolution parameters are

$$A = (2.15 \pm 0.01)\sqrt{\text{GeV}}, \quad B = 0 \text{ GeV}, \quad C = (5.8 \pm 0.2) \%. \quad (3.6)$$

The stochastic term is larger compared to previously tested readout systems [3] which can be attributed to the common bias voltage applied to all SiPMs. The noise term is consistent with zero.

4 Conclusion

While primarily intended for the readout of gas detectors, the VMM ASIC can be adapted for usage with silicon photomultipliers. The presented results confirm its applicability for calorimetry where a higher dynamic range is required and larger number of channels are active within a single event. The VMM dynamic range imposes restrictions on the measurable energy range and resolution, but by splitting the signal charge into two VMM channels with a charge division of 16:1 the effective dynamic range is extended accordingly. This principle was first implemented in a SiPM adapter board for the VMM with which the initial effects of channel saturation with single gain were successfully mitigated.

While the developed prototype adapter does not yet allow for individual adjustment of the bias voltage for each detector channel, an upgraded adapter could add functionality for individual channel tuning and current monitoring.

Acknowledgements

We would like to express our most sincere gratitude to the collaborating individuals, groups and organizations for their invaluable contributions to the success of the test beam campaigns mentioned in this document. We extend our appreciation to the staff and operators of the PS and

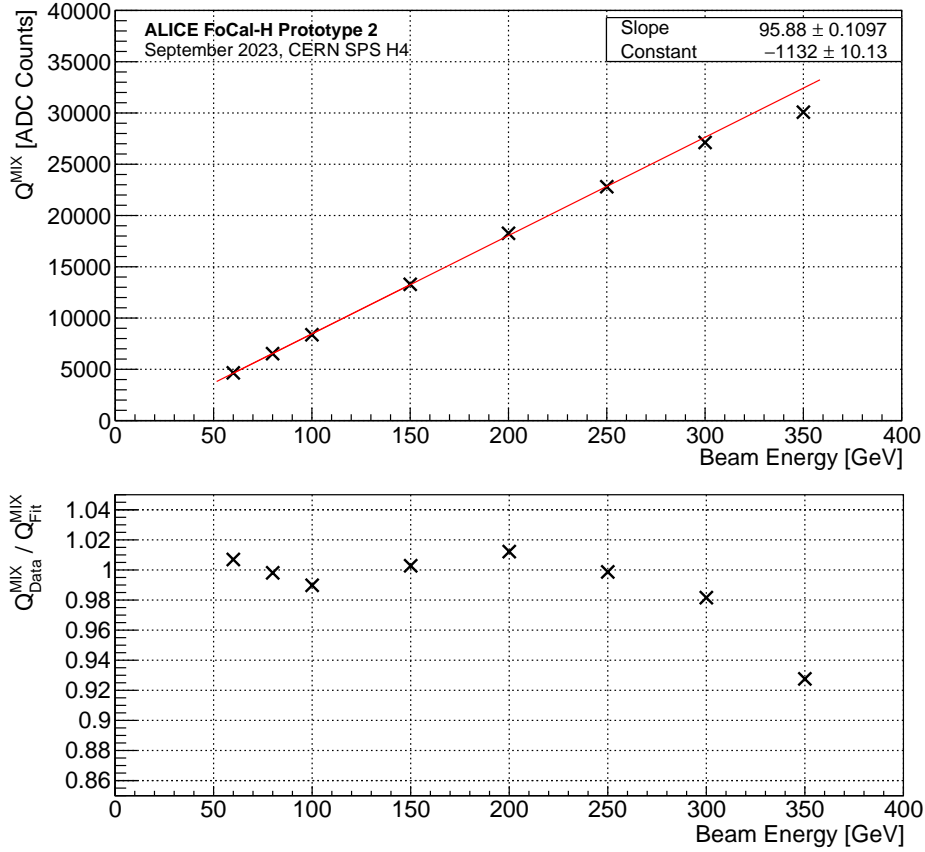


Figure 9. Top panel: Dependence of the mean values of Q^{MIX} as a function of the hadron beam energy. The linear fit is performed in the interval 60 GeV to 150 GeV and extrapolated to 350 GeV. Bottom panel: Ratios between the mean values of Q^{MIX} and the values predicted by the fit as a function of the hadron beam energy. SiPM bias voltage set to 55.4 V.

SPS test beam facilities at CERN for their assistance in setting up and conducting the experiment operations. I. Bearden, A. Buhl, L. Dufke and S. Jia acknowledge support from the The Carlsberg Foundation (CF21-0606) and the Danish Council for Independent Research/Natural Sciences. V. Kozhuharov and R. Simeonov acknowledge that partially this study is financed by the European Union-NextGenerationEU through the National Recovery and Resilience Plan of the Republic of Bulgaria, project SUMMIT BG-RRP-2.004-0008-C01. V. Buchakchiev acknowledges support from ESA through contract number 4000142764/23/NL/MH/rp.

References

- [1] *Letter of Intent: A Forward Calorimeter (FoCal) in the ALICE experiment*. Tech. rep. Geneva: CERN, 2020. URL: <https://cds.cern.ch/record/2719928>.
- [2] Collaboration ALICE. *Technical Design Report of the ALICE Forward Calorimeter (FoCal)*. Tech. rep. Geneva: CERN, 2024. URL: <https://cds.cern.ch/record/2890281>.

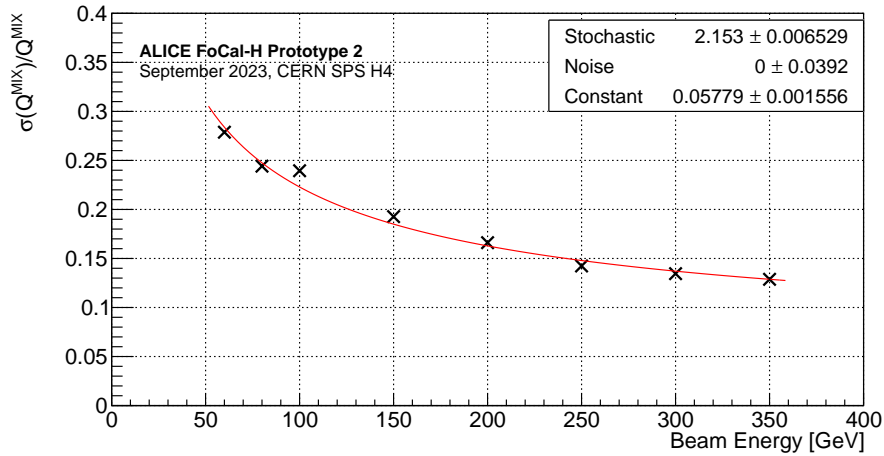


Figure 10. Dependence of the energy resolution obtained with LG/HG calibration on the hadron beam energy. SiPM bias voltage set to 55.4 V. The data is fit using Equation 3.5.

- [3] M. Aehle et al. “Performance of the electromagnetic and hadronic prototype segments of the ALICE Forward Calorimeter”. In: (2023). DOI: [10.48550/arXiv.2311.07413](https://doi.org/10.48550/arXiv.2311.07413). arXiv: [2311.07413](https://arxiv.org/abs/2311.07413) [physics.ins-det].
- [4] Sorin Martoiu et al. “Development of the scalable readout system for micro-pattern gas detectors and other applications”. In: *Journal of Instrumentation* 8 (2013), pp. 1–11. DOI: [10.1088/1748-0221/8/03/C03015](https://doi.org/10.1088/1748-0221/8/03/C03015).
- [5] L. Scharenberg et al. “Development of a high-rate scalable readout system for gaseous detectors”. In: *Journal of Instrumentation* 17.12 (Dec. 2022), p. C12014. DOI: [10.1088/1748-0221/17/12/C12014](https://doi.org/10.1088/1748-0221/17/12/C12014).
- [6] M. Lupberger et al. “Implementation of the VMM ASIC in the Scalable Readout System”. In: *Nuclear Instruments and Methods in Physics Research Section A: Accelerators, Spectrometers, Detectors and Associated Equipment* 903 (2018), pp. 91–98. ISSN: 0168-9002. DOI: [10.1016/j.nima.2018.06.046](https://doi.org/10.1016/j.nima.2018.06.046).
- [7] D. Pfeiffer et al. “Rate-capability of the VMM3a front-end in the RD51 Scalable Readout System”. In: *Nuclear Instruments and Methods in Physics Research Section A: Accelerators, Spectrometers, Detectors and Associated Equipment* 1031 (May 2022), p. 166548. ISSN: 0168-9002. DOI: [10.1016/j.nima.2022.166548](https://doi.org/10.1016/j.nima.2022.166548).
- [8] G. Iakovidis et al. “The New Small Wheel electronics”. In: *Journal of Instrumentation* 18.05 (May 2023), P05012. DOI: [10.1088/1748-0221/18/05/P05012](https://doi.org/10.1088/1748-0221/18/05/P05012).
- [9] CAEN. *CAEN A5253 3-pin header adapter for A5202/DT5202*. Last accessed: February 19th, 2024. URL: <https://www.caen.it/products/a5253/>.
- [10] Alexandru Rusu and Valentin Buchakchiev. *12bit Dynamic range SiPM readout with VMM3a at Focal test beam*. Tech. rep. 2023. URL: <https://indico.cern.ch/event/1327482/>

[contributions/5692929/attachments/2766718/4819360/VMM3a%20SiPM%20Readout.pdf](#).

- [11] L. Scharenberg et al. “Performance of the new RD51 VMM3a/SRS beam telescope — studying MPGDs simultaneously in energy, space and time at high rates”. In: *JINST* 18.05 (2023), p. C05017. DOI: [10.1088/1748-0221/18/05/C05017](#). arXiv: [2302.08330](#) [[physics.ins-det](#)].